

Electric fields and electron energies inferred from the ISUAL recorded sprites

Cheng-Ling Kuo,¹ R. R. Hsu,¹ A. B. Chen,¹ H. T. Su,¹ L. C. Lee,^{1,2} S. B. Mende,³ H. U. Frey,³ H. Fukunishi,⁴ and Y. Takahashi⁴

Received 1 May 2005; revised 16 August 2005; accepted 23 August 2005; published 5 October 2005.

[1] Electron energies and the strength of electric fields in sprites are deduced for five selected events, which were recorded by the space-borne instrument called ISUAL (Imager of Sprites and Upper Atmospheric Lightning; a payload on the FORMOSAT-2 satellite). From the derived peak intensity ratios of spectrophotometer channel 2 (centered at 337 nm) and channel 3 (centered at 391.4 nm) of these sprites, the average and characteristic electron energies were found to be in the range of 6.2–9.2 eV and 4.5–6.5 eV, respectively. The estimated E/N at 40–60 km is 243–443 Td and the strength of the electric field is 2.1–3.7 times that of the atmosphere breakdown E-field at these altitudes. The inferred electron energies and the strength of electric fields are about two times higher than those inferred from ground campaigns. However, they are consistent with the prediction of the sprite streamer model. **Citation:** Kuo, C.-L., R. R. Hsu, A. B. Chen, H. T. Su, L. C. Lee, S. B. Mende, H. U. Frey, H. Fukunishi, and Y. Takahashi (2005), Electric fields and electron energies inferred from the ISUAL recorded sprites, *Geophys. Res. Lett.*, 32, L19103, doi:10.1029/2005GL023389.

1. Introduction

[2] The characteristic red emission in sprites is from the N₂ first positive group (1PN₂) [Mende *et al.*, 1995; Hampton *et al.*, 1996; Green *et al.*, 1996]. Additional sprite emissions including N₂ second positive group (2PN₂) and N₂⁺ first negative group (1NN₂⁺) are also present [Armstrong *et al.*, 1998, 2000; Suszcynsky *et al.*, 1998], indicating that ionization processes exist in inducing these transient flashes. Emissions from sprites are associated with lightning-induced discharges, and they could reveal the conditions under which these optical flashes are created. For example, based on an aircraft spectral study, Morrill *et al.* [2002] inferred the characteristic electron energy and electric field inducing the observed sprite emissions.

[3] In this paper, the strength of electric fields and electron energies in ISUAL recorded sprites are deduced by matching a modeling results and ISUAL spectrophotometer data. To begin with, we solve the collisional Boltzmann kinetic equation by using the ELENDIF code [Morgan and Penetrante, 1990] to obtain the kinetic behavior of energetic electrons in weakly ionized plasma. The electron distribution

function, average electron energy, characteristic electron energy, and excitation rates of 2PN₂ and 1NN₂⁺ systems are calculated for E/N (E-field strength/gas density) between 20–600 Td (1 Townsend = 1E-17 volt-cm²). Considering the bandpasses of the ISUAL SP channels 2 and 3, the sprite emission intensities for SP channel 2 centered at 337 nm (2PN₂, 0-0) and SP channel 3 centered at 391.4 nm (1NN₂⁺, 0-0) were computed. The predicted peak intensity ratio of these SP channels can be obtained. By matching the modeling predictions of the ISUAL SP measured peak intensity ratios for several sprites, the magnitude of the electric field, the characteristic and average electron energies were derived.

2. The ISUAL Payload

[4] The FORMOSAT-2 satellite, which is the platform of the ISUAL payload, has a polar, sun-synchronous orbit of 891 km altitude. The ISUAL payload consists of an imager, a six-channel spectrophotometer (SP) and an array photometer (AP). The sprite images presented here were obtained through a 623–750 nm filter. The key photometric data are from channel 2 (centered at 337nm; bandwidth 5.6 nm) and channel 3 (centered at 391.4nm; bandwidth 4.2 nm) of the ISUAL SP. Other SP channels include SP1 (150–290 nm), SP4 (608.9–753.4 nm), SP5 (centered at 777.4 nm), and SP6 (228.2–410.2 nm). The ISUAL Imager, SP and AP are co-aligned at the center of their views. ISUAL Imager and SP are bore-sighted, and their field-of-view (FOV) is approximately 20 deg (H) × 5 deg (V). The sampling rate of ISUAL SP is 10 kHz. The ISUAL AP contains a blue (370–450 nm) and a red (530–650 nm) band multiple-anode photometers, that each AP has 16 vertically stacked PMTs with a combined FOV of 22 deg (H) × 3.6 deg (V) [Chern *et al.*, 2003; Mende *et al.*, 2005].

[5] The relative responses of ISUAL channels 2 (SP2) and 3 (SP3) are shown in Figures 1a and 1b. The overlaying bands are emissions from the 2PN₂ and 1NN₂⁺ systems. The intensity ratio of SP2/SP3 is chosen because both SP2 and SP3 are narrow band photometers that could minimize contamination from other emissions. Hence, the intensity ratio SP2/SP3 is relatively stable for observations from orbit. The intensity ratio between SP2 and SP3 has been demonstrated to be a sensitive quantity (V. P. Pasko, private communication, 2004), which can be used to estimate the E-field and the average electron energy in sprites.

3. The Projected Intensity Ratio of SP2/SP3

[6] The electron distribution function is obtained by solving a time-dependent Boltzmann solver for partially ionized plasma (ELENDIF) [Morgan and Penetrante,

¹Department of Physics, National Cheng Kung University, Tainan, Taiwan.

²National Applied Research Laboratories, Taipei, Taiwan.

³Space Sciences Laboratory, University of California, Berkeley, California, USA.

⁴Department of Geophysics, Tohoku University, Sendai, Japan.

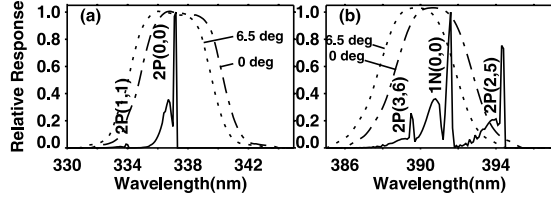


Figure 1. The relative responses of ISUAL SP (a) channel 2, (b) channel 3 for two different aspect angles. The relative band intensities are computed for E/N of 320Td and altitude of 60km, to analyze the band contributions for $2PN_2$ and $1NN_2^+$.

1990]. Using the cross section for $N_2(C^3\Pi_u)$ [Cartwright *et al.*, 1977] and $N_2^+(B^2\Sigma_u^+)$ [Borst and Zipf, 1970; Van Zyl and Pendleton, 1995], the excitation rates K_{ex}^α for upper state α of N_2 and N_2^+ molecules leading to $2PN_2$ and $1NN_2^+$ emissions (cm^3/sec) can be evaluated from

$$K_{ex}^\alpha = \frac{\nu_\alpha}{N} = \int_0^\infty v f(v) \sigma_\alpha(v) d^3v = \int_0^\infty \sqrt{\frac{2\varepsilon}{m_e}} n(\varepsilon) \sigma_\alpha(\varepsilon) d\varepsilon. \quad (1)$$

Here, ν_α is the excitation rate per electron leading to $2PN_2$ and $1NN_2^+$ emissions (sec^{-1}); σ_α is the electron impact excitation cross section of N_2 and N_2^+ molecules from the ground state to electronic state α (cm^2); N is the neutral density (cm^{-3}); v , ε , m_e are the electron velocity (cm/sec), energy (eV) and mass; $f(v)$ and $n(\varepsilon)$ are the normalized electron distribution functions that satisfy $\int_0^\infty f(v) d^3v = 1$ and $\int_0^\infty n(\varepsilon) d\varepsilon = 1$. The excitation rates for $N_2(C^3\Pi_u)$ and $N_2^+(B^2\Sigma_u^+)$, as functions of E/N (20–600 Td), are shown in Figure 2a. The population density of the upper states reaches its equilibrium value in a time of less than 10 ns, which is much shorter than the time resolution of SP (0.1 ms). Thus the emission intensity for the $2PN_2(0,0)$ and $1NN_2^+(0,0)$ bands, $n_{v'}^\alpha$, can be represented by their steady state form [Cartwright, 1978; Milikh *et al.*, 1998; Morrill *et al.*, 2002],

$$I_{v'}^{\alpha\beta} = n_{v'}^\alpha A_{v'}^{\alpha\beta} = N_{N_2} N_e A_{v'}^{\alpha\beta} \frac{K_{ex}^\alpha q_{0v'}^\alpha}{1/\tau_v^\alpha + (k_{q,v',O_2}^\alpha N_{O_2} + k_{q,v',N_2}^\alpha N_{N_2})}, \quad (2)$$

where N_e , N_{N_2} and N_{O_2} are electron, nitrogen and oxygen number densities (MSIS model) [Hedin, 1991]. Here $k_{q,v'}^\alpha$ is

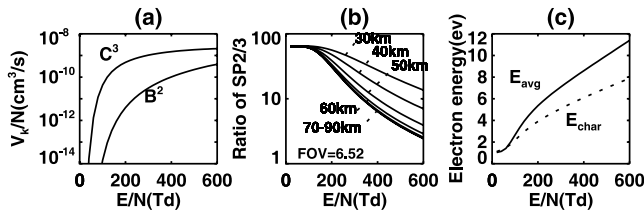


Figure 2. (a) The excitation rate for the upper state of $2PN_2 - C^3\Pi_u (C^3)$, and $1NN_2^+ - B^2\Sigma_u^+ (B^2)$, (b) the intensity ratio of SP2/SP3 as a function of E-field with aspect angle of 6.52 degree, and (c) the average electron energy (solid line) and the characteristic electron energy (dashed line) as a function of E/N .

the collisional quenching rate for the ν -th vibrational level of the α state. The Franck-Condon factor $q_{0v'}^\alpha$ is the transition probability from the 0-th vibrational level of the ground state χ to the ν -th vibrational level of the α state. The quantity $\tau_v^\alpha = (\sum_{\beta v'} A_{v\nu'}^{\alpha\beta})^{-1}$ is the lifetime of the ν -th vibrational level of the α state, where $A_{v\nu'}^{\alpha\beta}$ is the Einstein spontaneous transition probability from the ν -th vibrational level of the α state to the ν' -th vibrational level of the β state. The adapted values of these key parameters are listed in Table 1. In equation (2), $n_{v'}^\alpha$ is the number density of the ν -th vibrational level of the α state, which results from the direct excitation from the ground state to the ν -th vibrational level of the state α , but ignoring smaller cascading contribution from higher states. The projected and atmosphere attenuation corrected intensity in SP2 or SP3 is given by

$$I_{SP}(\theta) = \sum_\lambda T(\lambda) R(\lambda, \theta) I_{v\nu'}^{\alpha\beta}(\lambda), \quad (3)$$

where $T(\lambda)$ is the atmospheric transmittance, and $R(\lambda, \theta)$ is the response function of the ISUAL SP channels and dependent on the aspect angle θ of the sprite with respect to the center of FOV (Figure 1). The projected intensity ratio of SP2/SP3 is

$$\text{Ratio}(\theta) = I_{SP2}(\theta)/I_{SP3}(\theta). \quad (4)$$

To project the intensity that would be registered by SP2 and SP3, the emissions from $2PN_2(0,0)$ and $(1,1)$ are considered for SP2, and $2PN_2(2,5)$, $(3,6)$, and $1NN_2^+(0,0)$ are used for SP3 (Figure 1) with a Boltzmann temperature of 230 K [Morrill *et al.*, 1998; Herzberg, 1992]. The projected intensity ratio of S2/SP3 is a function of E/N and elevation and is sensitive to the aspect angle of the sprite (Figure 2b), which in turn can be used to infer the average and characteristic electron energies for a given altitude (Figure 2c).

4. Analysis of ISUAL Sprites

[7] Table 2 lists the observed and deduced characteristics of five ISUAL recorded sprite events. These sprite events were chosen because either they have clearly identifiable sprite emissions, or their parent lightning contributed negligibly to the ISUAL SP recorded signals. The background and lightning contributions have been subtracted from the listed peak and time-average intensities of SP2 and SP3.

[8] Figure 3 shows the time sequence of images for sprites recorded on 2004/07/18 at 21:30:15.316 (UT). The

Table 1. Key Parameters in Computing the Emission Bands $2PN_2(0-0)$ and $1NN_2^+(0-0)$

Parameter	$2PN_2(0-0)$	$1NN_2^+(0-0)$
τ_v^α (s)	$3.71E-8^{(a)}$	$6.23E-8^{(a)}$
$A_{v\nu'}^{\alpha\beta}$ (s^{-1})	$1.32E7^{(a)}$	$1.14E7^{(a)}$
$q_{0v'}^\alpha$	$0.545^{(a)}$	$0.883^{(a)}$
k_{q,v',O_2}^α (cc/s)	$2.85E-10^{(b)}$	$7.36E-10^{(b)}$
k_{q,v',N_2}^α (cc/s)	$1.12E-11^{(b)}$	$4.53E-10^{(b)}$

^aGilmore *et al.* [1992].

^bPancheshnyi *et al.* [1997]. At this value, the quench height for $2PN_2(0-0)$ and $1NN_2^+(0-0)$ band are 30 and 48 km.

Table 2. Observed and Deduced Parameters for Five Sprites^a

Trigger Time, UT	I_{SP2}	I_{SP3}	I_{SP2}/I_{SP3}	θ	E/N	ϵ_{avg}	ϵ_{char}	E/ E_k
2004/07/18 21:30:15.316(A) ^b	>134.30	9.30	>14.44	6.52	<302–<426	<7.1–<9.0	<5.1–<6.3	<2.6–<3.6
2004/07/18 21:30:15.316(B)	100.09	5.64	17.75	7.36	285–399	6.9–8.6	4.9–6.1	2.4–3.4
2004/10/22 16:23:45.081	57.10	2.85	20.04	5.14	252–347	6.3–7.8	4.6–5.6	2.1–2.9
2005/02/20 16:25:29.699	85.15	4.34	19.62	1.32	243–334	6.2–7.6	4.5–5.5	2.1–2.8
2005/03/06 23:22:30.623	49.76	4.31	11.55	2.89	313–443	7.3–9.2	5.2–6.5	2.6–3.7

^aUnit of I_{SP2} and I_{SP3} is 10^6 photons per square centimeter per second. θ is an aspect angle of incident light. E/N (Td) is calculated at 40–60 km. Unit of ϵ_{avg} and ϵ_{char} is eV. E_k is the breakdown electric field and is 118.5 Td [Papadopoulos et al., 1993].

^bThe peak I_{SP2} was saturated and more than 134.30. The inferred physical quantities are the upper limits.

corresponding intensities of six ISUAL SP channels with a time resolution of 0.1 ms are displayed in panels below the images. The zero point of the time axis in Figure 3 is the trigger time. The sprite marked as Event-A in Figure 3 is extremely bright, but it was also heavily contaminated by lightning emissions, which can be read in the signal profile of SP5. Mixing of sprite and lightning emissions is a norm. In analyzing the ISUAL spectrophotometer data, the lightning contribution needed to be properly subtracted.

[9] To show that the lightning contribution can be properly subtracted, the sprite event shown in Figure 3 is analyzed. Peaks AL and AS are the spectrophotometer peaks for the lightning and sprite in image frame A. Peak AL was from the sprite-inducing lightning and peak AS was mostly emitted by the sprite but with some lightning contaminations. Similarly, BL and BS denote the spectrophotometer peaks for the lightning and sprites in the image frame B. To obtain the lightning signals in peaks AL and BL as sensed by the ISUAL SP channels, background subtraction was performed first and then followed by a curve-fitting of exponential decay to determine the amount of lightning contribution under the sprite peaks. Figure 4 shows the residual SP signals from the sprite in frame A of Figure 3. That the peaks of SP1, SP4 are behind SP2, SP3 in Figure 4 indicates longer emission duration for SP1 and SP4, which are due to the relative long lifetime of the Lyman-Birge-Hopfield (LBH) and $1PN_2$ bands.

[10] The intensity ratios of SP2/SP3 for the lightning in image frame A and B are 0.50 and 0.46, respectively. Other ISUAL also have similar ratios. For the sprites in the same image frames, the peak intensity ratios of SP2/SP3 are 14.45 and 17.75, both are more than an order of magnitude higher than those for the lightning. As a result, the $1NN_2^+$ (0, 0) emission in SP3 is stronger than the $2PN_2$ emission in SP2. Thus for lightning, the ISUAL recorded SP2/SP3 ratio is always less than unity. Therefore, the intensity ratio of SP2/SP3 is a good indicator to distinguish sprites (>1) from lightning (<1). These results are also consistent with those from ground observations, although the selection of the photometric bands was slightly different [Armstrong et al., 1998]. With the observed peak intensity ratios of SP2/SP3, the physical parameters in sprites can be deduced using the prescription detailed in the previous section and the quantities are listed in Table 2.

5. Results, Discussion, and Summary

[11] Table 2 shows the peak intensity and the peak intensity ratio of SP2 and SP3 for five sprites. E/N could be determined with the intensity ratio SP2/SP3 using the functional curve in Figure 2b. E/N can be further converted into average and characteristic electron energies using the relationship shown in Figure 2c. The main uncertainty in the estimated E/N and electron energies arises from the uncertainty in determining the altitude of the sprite peak emission. Using the associated ISUAL array photometer recording, the altitude range of the major emission peaks of

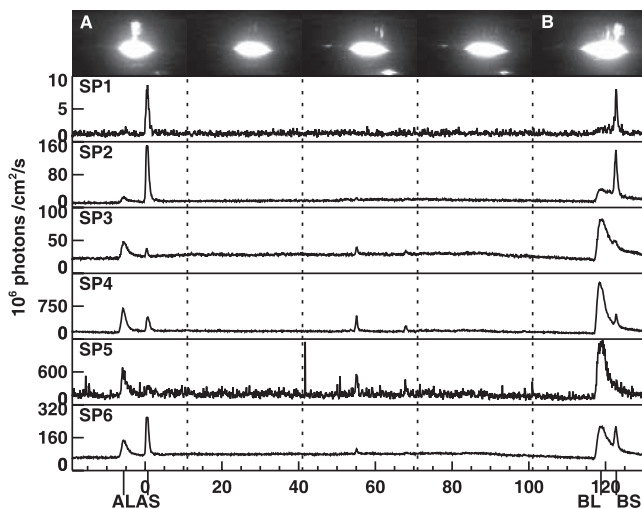


Figure 3. The selected frames for dancing sprites from ISUAL recorded at 2004/07/18 21:30:15.316 UT (top panel). The lower panels are signal traces from the six ISUAL SP channels.

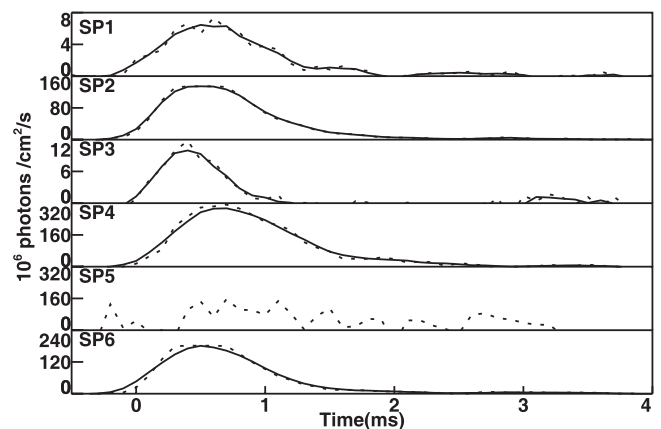


Figure 4. The residual emissions in the ISUAL SP from the sprite in frame A of Figure 3 after lightning and the background contributions have been removed. The solid lines are the smoothing curves of SP signals (dashed lines).

the reported sprites is from 40 to 60 km. With this peak emission altitude, the estimated E/N is 243–443 Td (2.1–3.7 E/E_k), the derived average electron energies are 6.2–9.2 eV, and the characteristic energies are 4.5–6.5 eV. These ratios infer higher values of E/N, electron energies and E/E_k at lower altitude (<40km) but nearly constant values at higher altitude (>60km) because of quenching effect.

[12] Morrill *et al.* [2002] reported that the estimated characteristic electron energy was ~2.2eV for their aircraft recorded sprites. Their estimate was based on the spectral intensity ratio between 2PN₂ (0, 0) and 1NN₂⁺ (0, 1), since the 1NN₂⁺ (0, 0) emission is severely absorbed at the aircraft observing altitude of 15 km. Their E_{ch} is much lower than the 4.5 to 6.5 eV reported here. The difference could be due to the averaging effect over various energetic streamers in their ~17 ms observation window.

[13] In modeling sprite streamers, Liu and Pasko [2005] reported that the electric field at the sprite streamer tip can be less than 3E_k. The strong optical emission is confined to the streamer head with a much darker streamer channel. Any spatially integrated optical signal will therefore be an average of the streamer tip luminosity as it moves through the FOV of the instrument. Our result is inferred from the peak luminosity (100 microsecond average), and is therefore consistent with the results of these recent streamer modeling results.

[14] In summary, five selected ISUAL sprites are studied and the physical parameters in the luminous regions are deduced. The derived average and characteristic electron energies are 6.2–9.2 eV and 4.5–6.5 eV, respectively. The estimated E/N at 40–60 km is 243–443 Td and the E/E_k is 2.1–3.7. These physical quantities are about two times higher than those from the ground observation [Morrill *et al.*, 2002], but are consistent with the theoretical prediction of the sprite streamer model [Liu and Pasko, 2005].

[15] **Acknowledgments.** We thank Victor P. Pasko, David D. Sentman, and J. Morrill for fruitful discussions. Works performed at NCKU are partially supported by grants 94-NSPO(B)-ISUAL-FA09-01 and NSC93-2112-M006-007.

References

- Armstrong, R. A., J. A. Shorter, M. J. Taylor, D. M. Suszcynsky, W. A. Lyons, and L. S. Jeong (1998), Photometric measurements in the SPRITES '95 & '96 campaigns of nitrogen second positive (399.8 nm) and first negative (427.8 nm) emissions, *J. Atmos. Sol. Terr. Phys.*, *60*, 787–799.
- Armstrong, R. A., D. M. Suszcynsky, W. A. Lyons, and T. E. Nelson (2000), Multi-color photometric measurements of ionization and energies in sprites, *Geophys. Res. Lett.*, *27*, 653–656.
- Borst, W. L., and E. C. Zipf (1970), Cross section for electron-impact excitation of the (0,0) first negative band of N₂⁺ from threshold to 3 keV, *Phys. Rev. A*, *1*, 834–840.
- Cartwright, D. C. (1978), Vibrational populations of the excited states of N₂ under auroral conditions, *J. Geophys. Res.*, *83*, 517–531.
- Cartwright, D. C., S. Trajmar, A. Chutjian, and W. Williams (1977), Electron impact excitation of the electronic states of N₂. II. Integral cross sections at incident energies from 10 to 50 eV, *Phys. Rev. A*, *16*, 1041–1051.
- Chern, J. L., R. R. Hsu, H. T. Su, S. B. Mende, H. Fukunishi, Y. Takahashi, and L. C. Lee (2003), Global survey of upper atmospheric transient luminous events on the ROCSAT-2 satellite, *J. Atmos. Sol. Terr. Phys.*, *65*, 647–659, doi:10.1016/S1364-6826(02)00317-6.
- Gilmore, F. R., R. R. Laher, and P. J. Espy (1992), Franck-Condon factors, r-centroids, electronic transition moments, and Einstein coefficients for many nitrogen and oxygen band systems, *J. Phys. Chem. Ref. Data*, *21*, 1005–1107.
- Green, B. D., M. E. Fraser, W. T. Rawlins, L. Jeong, W. A. M. Blumberg, S. B. Mende, G. R. Swenson, D. L. Hampton, E. M. Wescott, and D. D. Sentman (1996), Molecular excitation in sprites, *Geophys. Res. Lett.*, *23*, 2161–2164.
- Hampton, D. L., M. J. Heavner, E. M. Wescott, and D. D. Sentman (1996), Optical spectral characteristics of sprites, *Geophys. Res. Lett.*, *23*, 89–92.
- Hedin, A. E. (1991), Extension of the MSIS thermospheric model into the middle and lower atmosphere, *J. Geophys. Res.*, *96*, 1159.
- Herzberg, G. (1992), *Molecular Spectra and Molecular Structure I. Spectra of Diatomic Molecules*, p. 126, Krieger, Melbourne, Fla.
- Liu, N., and V. P. Pasko (2005), Molecular nitrogen LBH band system far-UV emissions of sprite streamers, *Geophys. Res. Lett.*, *32*, L05104, doi:10.1029/2004GL022001.
- Mende, S. B., R. L. Rairden, G. R. Swenson, and W. A. Lyons (1995), Sprite spectra; N₂ 1 PG band identification, *Geophys. Res. Lett.*, *22*, 2633–2636.
- Mende, S. B., H. U. Frey, R. R. Hsu, H. T. Su, A. B. Chen, L. C. Lee, Y. Takahashi, and H. Fukunishi (2005), D region ionization by lightning induced EMP, submitted to *J. Geophys. Res.*
- Milikh, G., J. A. Valdivia, and K. Papadopoulos (1998), Spectrum of red sprites, *J. Atmos. Sol. Terr. Phys.*, *60*, 907–915.
- Morgan, W. L., and B. M. Penetrante (1990), ELENDF: A time-dependent Boltzmann solver for partially ionized plasmas, *Comput. Phys. Commun.*, *58*, 127–152.
- Morrill, J., E. Bucseles, V. Pasko, S. Berg, M. Heavner, D. Moudry, W. Benesch, E. Wescott, and D. Sentman (1998), Time resolved N₂ triplet state vibrational populations and emissions associated with red sprites, *J. Atmos. Sol. Terr. Phys.*, *60*, 811–829.
- Morrill, J., *et al.* (2002), Electron energy and electric field estimates in sprites derived from ionized and neutral N₂ emissions, *Geophys. Res. Lett.*, *29*(10), 1462, doi:10.1029/2001GL014018.
- Pancheshnyi, S. V., S. M. Starikovskaya, and A. Y. Starikovskii (1997), Measurements of the rates of quenching of N₂(C³Π_u) and N₂(B²Σ_u⁺) states by N₂, O₂, and CO molecules in the afterglow plasma of a nanosecond discharge, *Plasma Phys. Rep.*, *23*, 616–620.
- Papadopoulos, K., G. Milikh, A. Gurevich, A. Drobot, and R. Shanny (1993), Ionization rates for atmospheric and ionospheric breakdown, *J. Geophys. Res.*, *98*, 17,593–17,596.
- Suszcynsky, D. M., R. Roussel-Dupr, W. A. Lyons, and R. A. Armstrong (1998), Blue-light imagery and photometry of sprites, *J. Atmos. Sol. Terr. Phys.*, *60*, 801–809.
- Van Zyl, B., and W. Pendleton (1995), N₂⁺ (X), N₂⁺ (A), and N₂⁺ (B) production in e⁻+ N₂ collisions, *J. Geophys. Res.*, *100*, 23,755–23,762.

A. B. Chen, R. R. Hsu, C.-L. Kuo, L. C. Lee, and H. T. Su, Department of Physics, National Cheng Kung University, No. 1 Ta-Hsueh Road, Tainan 701, Taiwan. (johnny@phys.ncku.edu.tw)

H. U. Frey and S. B. Mende, Space Sciences Laboratory, University of California, Berkeley, Centennial Drive at Grizzly Peak Boulevard, Berkeley, CA 94720-7450, USA.

H. Fukunishi and Y. Takahashi, Department of Geophysics, Tohoku University, Aramaki-aoba, Aoba-ku, Sendai, 980-8578, Japan.